Journal of Alloys and Compounds 688 (2016) 456–462

Contents lists available at ScienceDirect

Journal of Alloys and Compounds

journal homepage: http://www.elsevier.com/locate/jalcom

Effect of Zener-Hollomon parameter on quench sensitivity of 7085 aluminum alloy

Chengbo Li [a, b, c], Shaolin Wang [a, b], Duanzheng Zhang [a, b], Shengdan Liu [a, b, *], Zhaojun Shan [a, b], Xinming Zhang [a, b]

[a] School of Materials Science and Engineering, Central South University, Changsha, 410083, China
[b] Key Laboratory of Non-ferrous Metals Science and Engineering, Ministry of Education, Changsha, 410083, China
[c] Light Alloy Research Institute, Central South University, Changsha, 410083, China

A R T I C L E I N F O

Article history:
Received 14 April 2016
Received in revised form
6 July 2016
Accepted 7 July 2016
Available online 9 July 2016

Keywords:
Zener-Hollomon parameter
Quench sensitivity
7085 Al alloy
Dispersoids
Recrystallization

A B S T R A C T

The effect of Zener-Hollomon (Z) parameter on quench sensitivity of 7085 aluminum alloy was investigated. With the increase of Z parameter from 2.67E10 to 4.79E16, quench sensitivity relative to hardness tends to decrease first and then increase, and it may be minimised in the range from 2.67E12 to 2.24E13. The reason was discussed mainly on the effect of Z parameter on recrystallization fraction, which changes the amount of nucleation sites of heterogeneous precipitation during slow quenching. Quench-induced η phase with little strengthening effect tends to form preferentially at grain boundaries and on the Al_3Zr dispersoids with a size larger than about 23 nm in the recrystallized grains. The increase in the number of recrystallized grains can increase the amount of such grain boundaries and Al_3Zr dispersoids, and therefore a larger amount of quench-induced phase; consequently, quench sensitivity increases.

1. Introduction

7XXX (Al-Zn-Mg-Cu) series aluminum alloys are often quench sensitive, i.e, their properties tend to decrease with the decrease of cooling rate after solution heat treatment [1–4]. Consequently, quench-induced inhomogeneity of microstructure and properties is present inevitably in semi-products with large section of these alloys [5–7], because the cooling rate is often lower in the center layer than in the surface layer. In order to minimize the inhomogeneity, it is desirable to decrease quench sensitivity. It is known that chemical compositions have great influence on quench sensitivity. For instance, the increase of Zn, Mg and Cu content tends to increase quench sensitivity [8]; the alloys with a higher Zn/Mg ratio tend to be less quench sensitive [7]; the alloys with trace Zr are generally less quench sensitive than those with trace Cr [9]. Therefore, some alloys such as 7050, 7010 and 7085 with low quench sensitivity have been developed by the design of chemical compositions.

Moreover, apart from chemical compositions, microstructure is another important factor that may exert significant effect on quench sensitivity of 7XXX aluminum alloys. It is generally believed that quench sensitivity is closely related to the quantity of nucleation sites available for heterogeneous precipitation during slow quenching [10,11]. A larger quantity of such sites can lead to a larger quantity of quench-induced phase, which leads to fewer η′ strengthening precipitates in the matrix after subsequent aging; as a result, there is a larger decrement of hardness and strength due to slow quenching, i.e., quench sensitivity is higher. In 7XXX aluminum alloys with Zr, such nucleation sites seem to be primarily Al_3Zr dispersoids, subgrain and grain boundaries [4,10,12,13]. Hot deformation is a critical step in the production of semi-products of 7XXX aluminum alloys and may have significant effect on quench sensitivity by changing these microstructural features. For instance, in a 7050 aluminum alloy sheet, the increase of hot rolling reduction or deformation rate results in a larger fraction of recrystallization and quantity of incoherent Al_3Zr dispersoids, and consequently gives rise to higher quench sensitivity [14]. Therefore, it is possible to decrease quench sensitivity by optimizing hot deformation parameters, and this is based on good understanding of their effect on quench sensitivity.

7085 aluminum alloy is a typical alloy with low quench

* Corresponding author. School of Materials Science and Engineering, Central South University, Changsha, 410083, China.
E-mail addresses: csuliusd@163.com, lsd_csu@csu.edu.cn (S. Liu).

http://dx.doi.org/10.1016/j.jallcom.2016.07.089
0925-8388/

sensitivity [15]. In this work, the effect of Zener-Hollomon (Z) parameter on quench sensitivity of this alloy has been investigated. The Z parameter indicates the combined effect of two variables $\dot{\varepsilon}$ and T in the hot working process, and can be calculated by Eq. (1) [16],

$$Z = \dot{\varepsilon}\exp\left(\frac{Q}{RT}\right) \tag{1}$$

where $\dot{\varepsilon}$ is strain rate, T is temperature, R is the universal gas constant, Q is the apparent activation energy.

2. Experimental

The material was a 7085 aluminum alloy ingot fully-homogenized by heating slowly to 470 °C and holding for 24 h in an air furnace, and the chemical compositions were (wt%): 7.59 Zn, 1.65Mg, 1.54Cu, 0.11Zr, Fe < 0.08,Si < 0.06. The experimental procedures are showed in Fig. 1. Specimens with a size of Φ10 × 15 mm were cut from the homogenized ingot for hot compression, which was performed on a Gleeble-3500 machine at the temperatures from 300 °C to 450 °C with strain rates from 0.01 s^{-1} to 10 s^{-1}. The specimens were heated rapidly to the desired temperature, held for 2 min, compressed to a true strain of 0.7, and then immediately cooled in room temperature water. The Z parameters for various hot deformation conditions were calculated by Eq. (1), and Q value for the studied 7085 aluminum alloy was determined to be 172.0 kJ/mol.

The deformed specimens were solution heat treated at 470 °C for 1 h in an air furnace, and then quenched in room temperature water and still air. Some specimens were prepared for the measurement of cooling rate. A small hole was drilled to the center part of these specimens to insert a thermocouple (see Fig. 2) to record the time-temperature data during quenching. Three tests were made to obtain reliable data. According to these data, a high cooling rate of about 960 °C/s and a very low cooling rate of 1.8 °C/s were obtained for quenching in room temperature water and still air, respectively. After quenching, the specimens were immediately subjected to a two step artificial aging of 120 °C/5 h + 163 °C/16 h in an air-circulating furnace.

During quenching, the cooling rate may be different at different positions in the specimen; moreover, inhomogeneous deformation often occurs at the vertical section of the specimen and the central part may indicate the microstructure features after hot compression well. Therefore, the central part (the gray region showed in Fig. 2) of the specimens were cut for subsequent hardness testing and microstructure examination. For hardness testing, two samples were used to obtain reliable results. After grinding and polishing, the hardness was measured using a HV-10B hardmeter with a load of 3 kgf; three tests were made on each sample because scatter was small and finally an average hardness was calculated. Some samples were prepared by standard metallographical method, etched in a solution containing 1 ml HF, 16 ml HNO_3, 3 g CrO_3 and 83 ml H_2O and then observed on an XJP-6A optical microscopy to examine grain structure. Some samples were thinned carefully to foils with a thickness of about 0.1 mm, punched into small disks of 3 mm in diameter, and then electropolished in a solution containing 30% HNO_3 and 70% CH_3OH below −20 °C. They were examined on a Tecnai G^2 F20 S-Twin scanning transmission electron microscopy (STEM) with a high angle annular dark field (HAADF) detector and probe corrector operated at 200 kV.

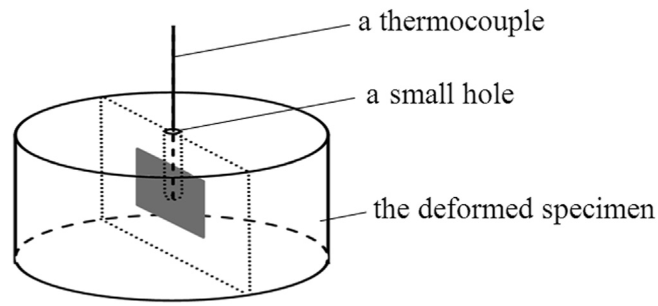

Fig. 2. Schematic of the specimen for measurement of cooling rate and the position (gray region) in the specimen for hardness testing and microstructure examination.

3. Results

3.1. Hardness and quench sensitivity

Fig. 3 (a) shows the effect of Z parameter on the hardness of the aged specimens. For both the rapidly-cooled and slowly-cooled specimens, the hardness tends to increase first with the increase of Z parameter and then decrease gradually, and the highest hardness can be seen at around Z = 2.24E12. The hardness of the slowly-cooled specimens is lower than that of the rapidly-cooled ones. The decrement of hardness, D, due to the decrease of cooling rate is defined here by Eq. (2) to describe the degree of quench sensitivity,

$$D = 100\% \times (H(960) - h(1.8))/H(960) \tag{2}$$

H(960) and h(1.8) are the hardness of the aged specimens cooled at 960 °C/s and 1.8 °C/s after solution heat treatment, respectively. Considering the deviation of hardness, the maximum and minimum D were calculated by Eq. (3) and Eq. (4).

$$D_{max} = 100\% \times \left(H(960)_{ul} - h(1.8)_{ll}\right)/H(960)_{ul} \tag{3}$$

$$D_{min} = 100\% \times \left(H(960)_{ll} - h(1.8)_{ul}\right)/H(960)_{ll} \tag{4}$$

$H(960)_{ul}$ and $H(960)_{ll}$ are the upperlimit and lowerlimit hardness of the aged specimens cooled at 960 °C/s, respectively. $h(1.8)_{ul}$ and $h(1.8)_{ll}$ are the upperlimit and lowerlimit hardness of the aged specimens cooled at 1.8 °C/s, respectively.

Fig. 3 (b) shows the effect of Z parameter on D_{max} and D_{min}. On the whole, D tends to decrease slightly first and then increase with the increase of Z parameter. A larger D indicates a larger decrement of hardness due to the decrease of cooling rate and therefore higher quench sensitivity. The largest D_{min} and D_{max} from 9.8% to 13.6% can be seen at Z = 4.79E16, which means the highest quench sensitivity under this hot deformation condition. It seems that the smallest D and D_{min} can be obtained with Z parameter ranging from 2.67E12 to 2.24E13. Therefore, it is likely that hot deformation with Z parameter in this range may minimize quench sensitivity of 7085

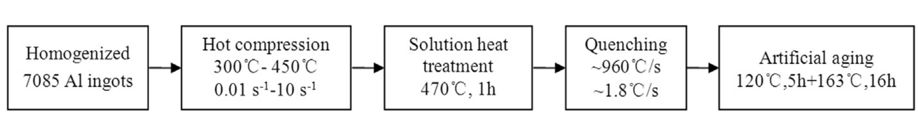

Fig. 1. Schematic of the experimental procedures.